Research Square

Preprints are preliminary reports that have not undergone peer review.
They should not be considered conclusive, used to inform clinical practice,
or referenced by the media as validated information.

# A perfusion method intensifies the production of polyhydroxyalkanoates from low concentrated volatile fatty acids

**Steven Leonhardt**
IGB: Fraunhofer-Institut fur Grenzflachen- und Bioverfahrenstechnik IGB
**Birk Achenbach**
University of Stuttgart: Universitat Stuttgart
**Pravesh Tamang**
IGB: Fraunhofer-Institut fur Grenzflachen- und Bioverfahrenstechnik IGB
**Alexander Beck**
IGB: Fraunhofer-Institut fur Grenzflachen- und Bioverfahrenstechnik IGB
**Günter M. E Tovar**
University of Stuttgart: Universitat Stuttgart
**Susanne Zibek**
susanne.zibek@igvp.uni-stuttgart.de

Universität Stuttgart: Universitat Stuttgart

**Research Article**

**Keywords:** Polyhydroxyalkanoates, PHA, Volatile fatty acid, VFA, Perfusion, Cupriavidus necator, growth kinetic, cell retention, bioreactor, ammonium inhibition, TFF

**Posted Date:** November 25th, 2026

**DOI:** https://doi.org/10.21203/rs.3.rs-11761241/v1

**License:** This work is licensed under a Creative Commons Attribution 4.0 International License.
Read Full License

# A perfusion method intensifies the production of polyhydroxyalkanoates from low concentrated volatile fatty acids

*Steven Leonhardt[1,2 +], Birk Achenbach[1,2], Pravesh Tamang[2], Alexander Beck[2,†], Günter M. E Tovar[1,2], Susanne Zibek[1,2]*

[1]Institute of Interfacial Process Engineering and Plasma Technology IGVP, University of Stuttgart, Pfaffenwaldring 31, 70569 Stuttgart, Germany

[2]Fraunhofer Institute for Interfacial Engineering and Biotechnology IGB, Nobelstr. 12, 70569 Stuttgart, Germany

[+]Current Adress: Institute of Bioprocess Engineering and Pharmaceutical Technology IBPT, TH Mittelhessen University of Applied Sciences, Germany

†Current Adress: SPIE Life Science Engineering GmbH, Ingersheimer Straße 10, 70499 Stuttgart, Germany

**Correspondence:**

Dr.-Ing. Susanne Zibek

susanne.zibek@igvp.uni-stuttgart.de

**Keywords:**

*Polyhydroxyalkanoates, PHA, Volatile fatty acid, VFA, Perfusion, Cupriavidus necator, growth kinetic, cell retention, bioreactor, ammonium inhibition, TFF*

# 1 Abstract

The sustainable production of polyhydroxyalkanoates (PHAs) from waste-derived volatile fatty acids (VFAs) offers a promising approach for advancing circular bioeconomy concepts. However, mixed VFA-containing streams are typically available only with low VFA concentrations (1–39 $g \cdot L^{-1}$), which may necessitate larger reactor volumes to achieve high PHA titers and can complicate process operations. To overcome these limitations, we designed a perfusion process based on tangential flow filtration (TFF), which is intended to enable continuous cell retention during PHA production by *Cupriavidus necator* H16, which is cultured on a mixture of VFAs.

To establish the biological and engineering fundamentals basis for perfusion cultivation, microbial growth kinetics on VFAs and ammonium were characterized along with the filtration performance of the TFF membrane. A critical membrane flux between $4.0 \cdot 10^{-7}$ and $4.6 \cdot 10^{-7}$ m $s^{-1}$ was identified, providing an upper limit for stable operating conditions required for prolonged cultivations. The developed perfusion strategy was subsequently demonstrated in 3.6 L bioreactor experiments using synthetic mixture of VFAs as the sole carbon source. With a feed medium containing 20 $g \cdot L^{-1}$ VFAs, the process achieved a PHA titer of 4.2 ± 0.2 $g \cdot L^{-1}$, a productivity of 0.12 $g \cdot L^{-1} \cdot h^{-1}$, and a substrate conversion efficiency of 0.13 $g_{PHA} \cdot g^{-1}_{VFA}$. To the best of our knowledge, these performance indicators exceed the results of previous studies in which comparable batch fermentations were carried out using mixed VFA feedstocks.

Overall, this work demonstrates the technical feasibility of TFF-based perfusion cultivation for increasing PHA production from inhibitory VFA mixtures. It also provides key design parameters for process operation. The proposed strategy thus represents an important step towards the efficient valorization of VFAs derived from waste-streams and the sustainable production of bioplastics from renewable carbon sources.

## 2 Introduction

Volatile fatty acids (VFAs), or short-chain fatty acids (SCFAs), are a group of alkanoic acids with six or fewer carbon atoms that may be branched or unbranched. These organic acids are widely recognized as important platform chemicals and key intermediates in the emerging bioeconomy (Velghe et al., 2021). Consequently, their valorization is currently a subject of ongoing research efforts. Among the numerous valorization routes proposed for VFAs, microbial production of polyhydroxyalkanoates (PHAs) biopolyesters has attracted considerable attention. These biopolyesters are produced by various microorganisms, with *Cupriavidus necator* being the most researched. However, although the microbial conversion of VFAs to PHAs is well understood (Yu and Si, 2004) and high yields and productivities have been demonstrated under well-controlled laboratory conditions (Huschner et al., 2015), several challenges currently hinder an industrialization.

On one hand, the VFA-rich streams produced from processes such as anaerobic treatment or thermal hydrolysis of organic waste are typically available at relatively low concentrations, commonly ranging from 1 to 39 $g \cdot L^{-1}$ (Cheah et al., 2019; Jiang et al., 2013; Prakash et al., 2024). As a result, further steps to concentrate the VFAs are often required before these streams can be used efficiently in conventional fed-batch processes. On the other hand, VFAs exhibit inhibitory effects on microorganisms even at relatively low concentrations (Cai et al., 2023; Jawed et al., 2022; Leonhardt et al., 2025). For *Cupriavidus necator H16*, growth inhibition ($IC_{50}$) has been observed in our work previously at substrate concentrations ranging from 3.9 to 10.5 $g \cdot L^{-1}$ (Leonhardt et al., 2025). This creates a narrow operational window for a process design, as low substrate concentrations limit biomass and product formation, whereas higher concentrations inhibit cellular metabolism (Wang et al., 2010).

Consequently, conventional batch cultivation is generally restricted to low initial VFA concentrations, resulting in comparatively low product titers. Achieving industrially relevant

product quantities under these conditions requires large cultivation volumes and, therefore, large bioreactor vessels. Fed-batch cultivation can partially mitigate substrate inhibition by maintaining VFA concentrations below inhibitory levels through controlled substrate addition, as demonstrated by Huschner et al. (2015). However, when low-concentration VFA streams are used directly, substantial feed volumes are required to provide sufficient substrate. This ultimately increases the required reactor capacity and and associated capital expenditure.

Perfusion cultivation offers an attractive alternative as it enables continuous medium exchange which ensures constant substrate availability while maintaining low inhibitory VFA concentrations, thereby facilitating high cell density via cell retention system. Simultaneously, large volumes of dilute feedstock can be continuously fed without increasing the reactor volume, as already demonstrated by Kacanski et al. (2022) using acetic acid feed.

However, in our last study, we showed that feeding mixtures of VFA instead of single VFAs, may lead to multiphasic growth (Leonhardt et al., 2026). This phenomenon typically arises from the preferential consumption of specific VFAs, resulting in the sequential utilization of the available substrates. Consequently, successful implementation of continuous feeding strategies requires a detailed understanding of the effects of individual VFA species and ammonium concentrations on microbial growth, as well as precise control of substrate concentrations within the bioreactor.

In this study, we present a membrane-based perfusion process for PHA production from dilute mixed-VFA streams using a pH-stat feeding strategy with additional OUR-regulated pulse feeding. First, the tangential flow filtration membrane was comprehensively characterized, as stable process operation relies on the continuous removal of large volumes of spent medium. Particular emphasis was placed on identifying the critical membrane flux to define operational limits and minimize membrane fouling during long-term cultivation. Second, we investigate and model the influence of VFA and ammonium concentrations on microbial growth at pH

values suggested by Leonhardt et al. (2026). Finally, the developed perfusion strategy was evaluated for PHA production from low-concentration mixed VFA feedstocks.

# 3 Methods

### Microbial strain

The microorganism *Cupriavidus necator H16 was* used in this study. The strain has been provided by the German Collection of Microorganisms and Cell Cultures (DSMZ). For long term storage the strain was frozen to -80 °C on 16.5 % glycerol.

For cultivation, the microorganisms were streaked on LB agar plates. LB agar plates were stored at 4 °C for less than 3 weeks.

### Preculturing

For the first seed culture, *C. necator H16* was aseptically transferred from agar plates into 1 mL reaction tubes with LB medium (10 $g \cdot L^{-1}$ tryptone, 5 $g \cdot L^{-1}$ yeast extract, 5 $g \cdot L^{-1}$ sodium chloride). The culture was thoroughly mixed and transferred into a 100 mL baffled shake flask containing 20 mL LB medium. The shake flask was incubated at 120 rpm and 30 °C in an incubator shaker (Infors HT, Switzerland).

After 12 h the culture attained a late exponential growth phase and was used to inoculate the second seed culture to an optical density ($OD_{600}$) of 0.1. The medium used for the second preculturing was a modified Schlegel mineral salt medium (10 $g \cdot L^{-1}$ Fructose, 4.5 $g \cdot L^{-1}$ $Na_2HPO_4$, 1.5 $g \cdot L^{-1}$ $KH_2PO_4$, 4.4 $g \cdot L^{-1}$ $(NH_4)_2SO_4$, 0.05 $g \cdot L^{-1}$ ammonium ferric citrate, 0.01 $g \cdot L^{-1}$ $CaCl_2$ x $2H_2O$, 0.2 $g \cdot L^{-1}$ $MgSO_4$ x $7H_2O$, 1 $mL \cdot L^{-1}$ SL6 trace element solution). SL6 trace element solution consisted of 1 $g \cdot L^{-1}$ $ZnSO_4$ x $7H_2O$, 0.3 $g \cdot L^{-1}$ $MnCl_2$ x $4H_2O$, 3 $g \cdot L^{-1}$ $H_3BO_3$, 4 $g \cdot L^{-1}$ $CoCl_2$ x $6H_2O$, 0.1 $g \cdot L^{-1}$ $CuCl_2$ x $2H_2O$, 0.4 $g \cdot L^{-1}$ $NiCl_2$ x $6H_2O$, 0.3 $g \cdot L^{-1}$ $Na_2MoO_4$ x 2 $H_2O$. pH was adjusted to 7.0 with NaOH. The second preculture was incubated at 120 rpm and 30 °C in an incubator shaker for 16 h. Precultures were aseptically transferred to 50 mL

centrifuge tubes and centrifuged at 4,680 g for 20 min (Thermo Fisher Scientific, USA). Supernatant was discarded, while the cell pellet was resuspended in 10 mL sterile 0.9 % NaCl per tube. OD was measured. The suspension was further diluted with 0.9 % NaCl, if necessary, in order to inoculate shake flasks to an OD of 0.1 and bioreactors to an OD of 1 with 10 % of the final volume.

**Shake flask cultivations**

Kinetic experiments were performed in shake flasks for modelling influence of VFA and ammonium concentration onto growth rate at pH 7.5 which was previously identified as the optimal pH for growth (Leonhardt et al., 2026). Shake flasks were equipped with the SBI shake flask cultivation system (Scientific Bioprocessing Inc., USA). Biomass was monitored online using a multiparameter sensor (MPS) based on backscattered light measurements at a wavelength of 940 nm. Data acquisition was carried out at a sampling interval of 1 min throughout the entire cultivation. Cultivation conditions and mineral medium of preculture has been used in the cultivations. VFA and $(NH_4)_2SO_4$ concentrations have been varied to reach the total VFA and $NH_4^+$ concentration shown in Table 1.

*Table 1 Experimental set-up and kinetical modelling*

| | **VFA concentration** | **$NH_4$ concentration** | **Kinetical model** |
|---|---|---|---|
| **Growth kinetic of VFA** | 0.25 – 2.0 $g \cdot L^{-1}$ | 2.0 $g \cdot L^{-1}$ | Monod (1949) |
| **Growth kinetic of $NH_4$** | 0.5 $g \cdot L^{-1}$ | 0.1 – 2.0 $g \cdot L^{-1}$ | Han and Levenspiel (1988) |

Apparent growth rates $\mu_{app}$ were estimated by plotting on a semi-logharithmic scale and subsequent linear fitting, as described by Doran (1995) and Baranyi and Pin (1999). Influence of VFA mixture onto concentrations was modelled by Monod kinetic for non-inhibiting conditions as described by Eq. 1,

$$\mu_{app} = \frac{\mu_{max} \cdot c_{VFA}}{K_{VFA} + c_{VFA}} \quad (1)$$

and influence of $NH_4^+$ using Han-Levenspiel kinetic was used to describe inhibiting conditions (Eq. 2).

$$\mu_{app} = \mu_{max} \cdot \left(1 - \frac{c_{NH_4}}{c_{crit}}\right)^n \cdot \left(\frac{c_{NH_4}}{c_{NH_4} + K_{NH_4} \cdot \left(1 - \frac{c_{NH_4}}{c_{crit}}\right)^m}\right) \quad (2)$$

Kinetics have been fitted using professional graphing software Origin (OriginLab, USA). If not otherwise stated, default fitting parameters have been applied.

**Bioreactor operation and tangential flow filtration**

Bioreactor studies were performed using a laboratory scale bioreactor with a working volume of 3.6 L (Infors HT, Switzerland). The bioreactor was filled with 2.0 L medium. Additionally, the holdup volume of the TFF module was 1.2 L, adding up to a total reaction volume of 3.2 L. The bioreactor was operated at a stirrer speed of 200 rpm, with an aeration rate of 1 vvm and a controlled temperature of 30 °C. During the growth phase a pH of 7.5 was maintained by feeding VFA rich growth medium (see Figure 1, Red lines). The fed growth medium contained total VFA concentration of 20.1 $g \cdot L^{-1}$ (6.7 $g \cdot L^{-1}$ acetic acid, 8.6 $g \cdot L^{-1}$ propionic acid, 2.3 $g \cdot L^{-1}$ butyric acid, 0.7 $g \cdot L^{-1}$ iso-butyric acid, 1.2 $g \cdot L^{-1}$ valeric acid, and 0.6 $g \cdot L^{-1}$ iso-valeric acid) along with 4.5 $g \cdot L^{-1}$ $Na_2HPO_4$, 1.5 $g \cdot L^{-1}$ $KH_2PO_4$, 10.5 $g \cdot L^{-1}$ $(NH_4)_2SO_4$, 0.05 $g \cdot L^{-1}$ ammonium ferric citrate, 0.01 $g \cdot L^{-1}$ $CaCl_2$ x $2H_2O$, 0.2 $g \cdot L^{-1}$ $MgSO_4$ x $7H_2O$, 1 $mL \cdot L^{-1}$ SL6 trace element solution). SL6 trace element solution consisted of 1 $g \cdot L^{-1}$ $ZnSO_4$ x $7H_2O$, 0.3 $g \cdot L^{-1}$ $MnCl_2$ x

157 $4H_2O$, 3 g·L$^{-1}$ $H_3BO_3$, 4 g·L$^{-1}$ $CoCl_2$ x $6H_2O$, 0.1 g·L$^{-1}$ $CuCl_2$ x $2H_2O$, 0.4 g·L$^{-1}$ $NiCl_2$ x $6H_2O$,
158 0.3 g·L$^{-1}$ $Na_2MoO_4$ x 2 $H_2O$. At the beginning of the production phase, the pH was adjusted to
159 8.0 with 4 M NaOH, and the medium was replaced with a production medium. Production
160 medium was identical to the growth medium but was deficient in ammonium sulfate. The initial
161 medium in the bioreactor contained 0.26 g·L$^{-1}$ $(NH_4)_2SO_4$ and 0.5 g·L$^{-1}$ total VFA with the
162 same relative VFA composition as the feed media.

163 In the exhaust gas, oxygen and carbon dioxide were measured using the off-gas sensor
164 BlueVary (BlueSense, Germany). Oxygen uptake rate (OUR) was calculated according to Beck
165 et al. (2022) and Chmiel et al. (2018):

166

$$OUR = \frac{F_G \cdot p_G}{V_L \cdot R \cdot T} \cdot \left( {y_{O_2}}^{in} - \frac{1 - {y_{O_2}}^{in} - {y_{CO_2}}^{in}}{1 - {y_{O_2}}^{out} - {y_{CO_2}}^{in}} \cdot {y_{CO_2}}^{out} \right) \quad (3)$$

167

168 In addition to the pH-controlled feeding of the VFA rich, acidic medium, each decrease in the
169 OUR triggered the addition of an 80 mL pulse of nutrient medium together with 13 mL of 4 M
170 NaOH. This depicts an adapted variation of the pH-stat with $pO_2$ pulses demonstrated by
171 Huschner et al. (2015)and Achenbach et al. (2026).

172 An autoclaved solution of 10 % Polypropylene glycol with molar mass of 2000 g·mol$^{-1}$ was
173 used as an antifoam agent, which was employed manually by a syringe when necessary.
174 Additionally, mechanical foam breakers were installed in the head-space of the bioreactor.

175 Performing bioreactor cultivations in perfusion mode requires a system for cell separation and
176 retention (see Figure 1, Green lines). To ensure a scalable process later, for cell retention a
177 tangential flow filtration with a reusable ceramic membrane was employed. The membrane
178 module (atech innovations, Germany) consisted of seven channels, each with an inner diameter

of 6 mm, providing a filtration area of 1,320 cm². The size of the rod-shaped *C. necator N-1* has been reported to be 0.7 – 0.9 µm in width and 0.9 – 1.3 µm in length (Makkar and Casida, 1987). Therefore, pore size of 0.4 µm was used for the membrane, which resulted in optically clear permeates in preliminary experiments.

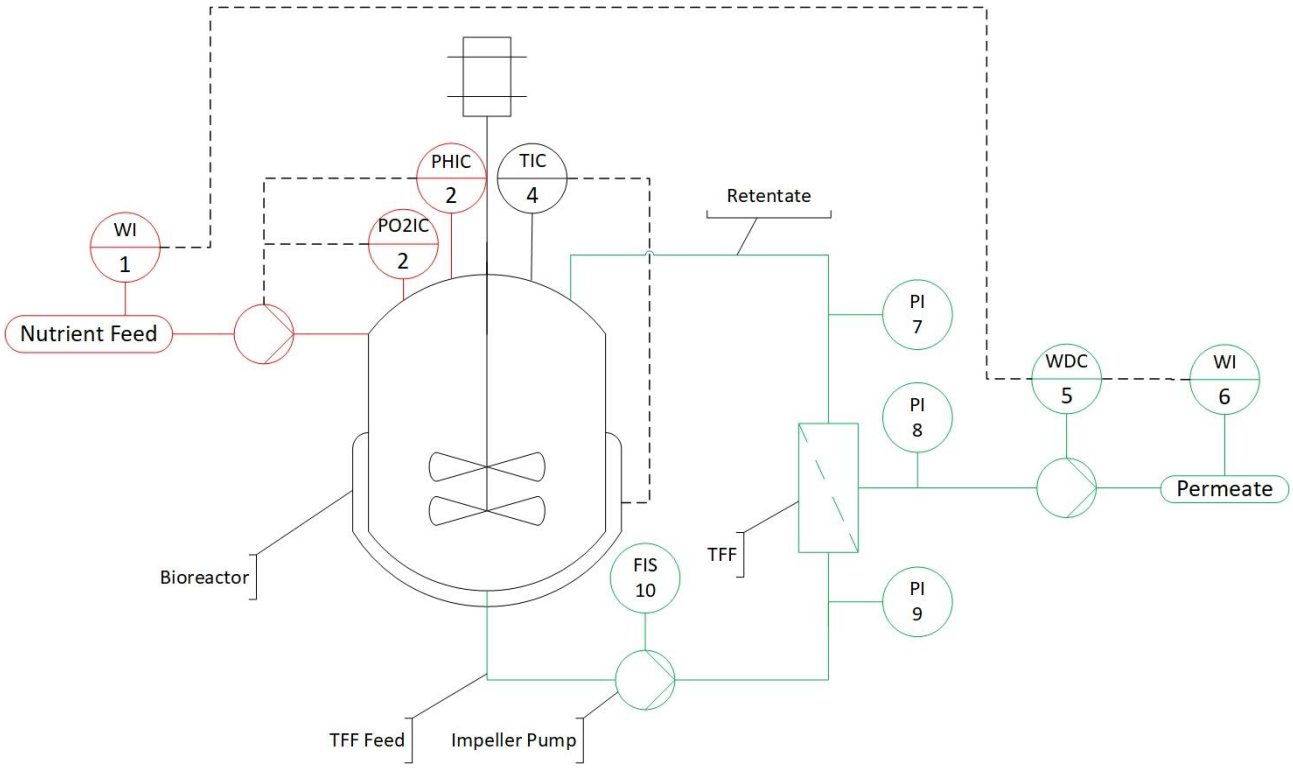


*Figure 1: P&ID of Bioreactor, Cell Retention and Control of Feeding. Feeding control is coloured red and the volume equivalent removal of liquid by TFF is coloured green.*

For feeding the TFF membrane, a Nirostar 2000-D/PF impeller pump (ZUWA, Germany) was used. A flow rate of 4 $L \cdot min^{-1}$ (equivalent to a linear velocity of 0.337 $m \cdot s^{-1}$) was applied for feeding of the TFF as this ensured a tubing *Reynolds number* of 2500 in the membrane. Therefore, a flow regime in the laminar–turbulent transition region was found in the membrane. In general, a turbulent regime is commonly seen to reduce fouling (Agrawal et al., 2023), however the increased shear stress might also be harmful to bacterial cells (Arnaud et al., 1993). In addition, we found that further increasing the flow rate to reach a turbulent regime leads to heat up of the medium, surpassing the cooling abilities of our reactor system. To control

permeate flow rate, a Watson Marlow 120 U peristaltic pump (Whatson Marlow, Great Britain) was used. Both pumps were controlled by a Labmanager automation system (HiTecZang, Germany). Flow rate of nutrient feed into the bioreactor was measured gravimetrically using a scale with an upper limit of 16 kg (Kern, Germany), while flow of permeate was measured by a 32.5 kg scale (Sartorius, Germany). Both scales were connected to the Labmanager automation system, providing online data of the feed streams for control of the permeate pump. As flow rate of the nutrition feed changed during the course of fermentation, a PI controller on the automation system was employed to ensure an equal flow rate of permeate to keep the volume of culture broth in the reactor steady. For precise calculation of mass balances, current weights were noted at the time of bioreactor sampling. Pressure in the TFF feed, retentate, and permeate was monitored using 0 – 4 bar manometers and manually noted during bioreactor sampling. The TFF module, associated fittings, and pumps were connected to the 6 mm ports of the bioreactor using fabric hoses. The TFF feed stream was drawn from beneath the liquid surface in the bioreactor via a PTFE tube, while a separate PTFE tube returned the retentate below the liquid surface to reduce foaming.

The TFF module and all fittings and instruments connected by fabric hoses were disinfected using the CIP protocol presented in Table 2.

*Table 2: CIP protocol for TFF module and connection to the bioreactor port*

| **Step Nr.** | **Duration** | **Agent** |
|---|---|---|
| 1 | 20 min | demineralized water |
| 2 | 20 min | 10 % citric acid |
| 3 | 20 min | demineralized water (sterile) |
| 4 | 20 min | 2 M NaOH |

| | | |
|---|---|---|
| 5 | 20 min | demineralized water (sterile) |
| 6 | 20 min | 70 % Ethanol |
| 7 | 20 min | demineralized water (sterile) |
| 8 | 20 min | demineralized water (sterile) |
| 9 | 20 min | demineralized water (sterile) |
| 10 | 10 min | Emptying the membrane with air through a 0.22 µm sterile filter. |

213

214 **Estimation of critical flux**

215 Critical flux $J_{crit}$ in $m^1 \cdot s^{-1}$is defined as the permeate flow in $m^3 \cdot s^{-1}$, normalized to membrane
216 surface area in $m^2$, above which any further increase results in a pronounced onset of fouling.
217 In Eq. 3 the relation of flux and pressure is described. In TFF the aim is to avoid filter cake
218 formation, thus filter resistance *R* remains roughly on the same value during filtration. However,
219 exceeding the critical flux, the filter cake can start to form on the filter, thus increasing *R*. As a
220 consequence, higher transmembrane pressures $\Delta p$ are required to form the same flux *J*. The
221 critical flux thus represents the transition between stable filtration with negligible fouling and
222 operating conditions where fouling rapidly accelerates, making it a key parameter for evaluating
223 membrane performance.

$$J = \frac{\Delta p}{\mu \cdot R} \tag{3}$$

224 The critical flux has been determined by a method adapted from Espinasse et al. (2002).
225 Experiments were conducted using *Cupriavidus necator H16* culture broth from second
226 preculture step. The set-up of the TFF module was analogue to the set up used for the perfusion
227 bioreactor study. Permeate flow rates were monitored using a 16 kg balance (Kern, Germany)

and controlled via a PI controller integrated into the LabManager automation system. Stepwise flux setpoints were applied for more than 4 min each and subsequently increased. After each flux step, the flow rate was returned to the initial setpoint for duration of 4 min to assess potential increases in filtration resistance. Pressure was measured using manometers.

### Analytical Methods

The analytical procedures for volatile fatty acids, PHA, cell dry weight and ammonium were performed as described by Leonhardt et al. (2026).

### Declaration use of AI

The large language model ChatGPT 5.2 was used exclusively for linguistic editing and readability improvement, as well as enhancement of the process visual representations in the graphical abstract of this manuscript under the supervision of the authors. No scientific content, interpretations, or conclusions were contributed by AI and remain the responsibility of the authors. The use of AI assistance thus followed the recommendations of the Committee on Publication Ethics (COPE) regarding the ethical use of AI in scholarly publishing.

## 4 Results and Discussion

In the following sections we first describe the characteristics of the tangential flow filtration (TFF) device used for cell retention. Subsequently, we investigated the growth kinetics and PHA production behaviour of *C. necator H16* at varying $NH_4^+$ and VFA concentrations. Lastly, we present data of the perfusion strategy in the final process configuration.

### 4.1 Characterization of tangential flow filtration

A ceramics-based membrane filter was used in the TFF device for the retention of biomass in the bioreactor. As reduction in permeate flow caused by fouling is a common problem in these

kinds of processes, the critical flux $J_{crit}$ was investigated. According to Espinasse et al. (2002) fouling is significantly reduced when performing filtration below this critical value. As previously described, we therefore performed experiments using culture broth, varying the permeate pump speed thus changing permeate flux $J$ and transmembrane pressure $\Delta p$. The results of the experiments are shown in Figure 2.

Figure 2A shows the time course of J and $\Delta p$. Applying fluxes below $4 \cdot 10^{-7}$ m·s$^{-1}$ showed no measurable increase in transmembrane pressure over time, indicating negligible membrane fouling. At J = $4.6 \cdot 10^{-7}$ m·s$^{-1}$, first signs of a change in the regime occurred as pressure increase from $0.11 \cdot 10^{6}$ Pa to $0.13 \cdot 10^{6}$ Pa within 1.5 min after applying the flux. However, at this setting the filtration stabilized after reaching this plateau.

At higher fluxes of $5.3 \cdot 10^{-7}$ m·s$^{-1}$ und $5.5 \cdot 10^{-7}$ m·s$^{-1}$ a constant increase of transmembrane pressure was observed, indicating a progressive blocking of the membrane. This ultimately also led to a decrease in flux as well, represented by high standard deviations in Figure 2B.

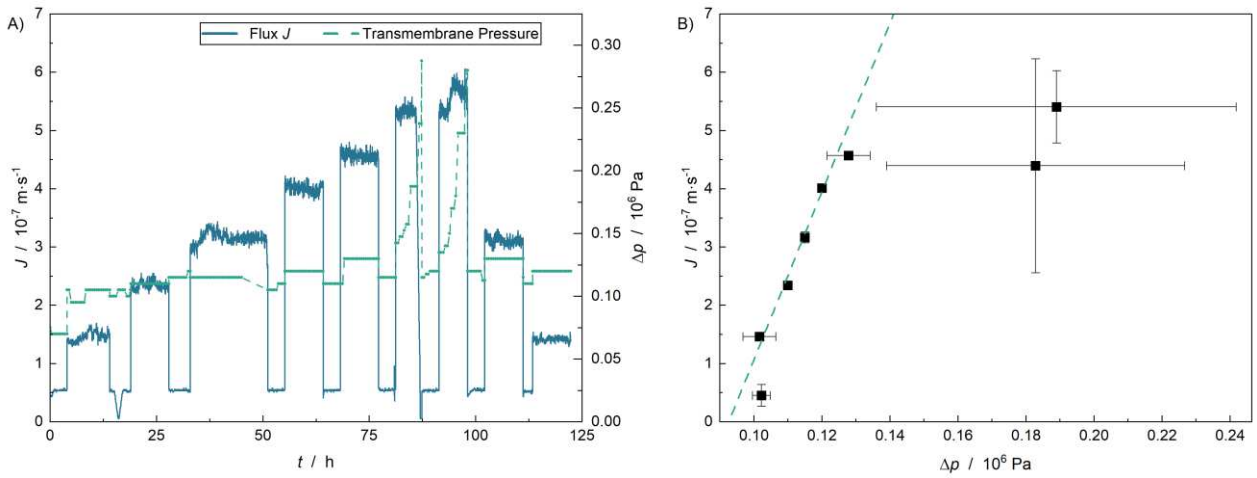


*Figure 2 Estimation of critical flux with A) evolution of permeate flux J and transmembrane pressure Δp; and B) showing the linear relationship between flux and transmembrane pressure for $\Delta p < 0.13 \cdot 10^{6}$ Pa.*

According to the Darcy equation (Eq. 3) a linear relation is to be expected in TFF as long as dynamic viscosity $\mu$ and filter resistance $R$ remain constant. However, during progressive

membrane fouling in TFF, deposited solids increase the filter resistance. As a result, $R$ is no longer constant, and the relationship between $J$ and $\Delta p$ becomes non-linear. Moreover, as shown by Espinasse et al. (2002), relevant fouling of filter membrane sets in, after J exceeds the critical Flux $J_{crit}$.

To identify the $J_{crit}$, where the relation deviates from linear behaviour, a linear regression was performed for $J < 5 \cdot 10^{-7}$ m·s$^{-1}$. As seen in Figure 2B, at $J = 4.6 \cdot 10^{-7}$ m·s$^{-1}$ $\Delta p$ increased, thus moving out of linear range during the test. Therefore, from Figure 2B the critical flux was estimated to be between $4.0 \cdot 10^{-7}$ m·s$^{-1}$ and $4.6 \cdot 10^{-7}$ m·s$^{-1}$. Considering the filtration surface area of the membrane used, critical permeate flow equates to 31.7 mL·min$^{-1}$. The pump used for feeding the bioreactor enables a flow of up to 10 mL·min$^{-1}$, thus no fouling was expected to be observed with the proposed setup in a steady state operation.

## 4.2 Characterization and modelling of *C. necator* H16 growth

To investigate the growth behaviour of *C. necator H16* at different VFA and ammonium concentrations under conditions relevant for perfusion cultivation, shake-flask experiments were performed at an initial pH of 7.5. Biomass accumulation was monitored online using backscatter measurements.

*C. necator H16* exhibits a complex growth behaviour when cultivated on a mixture of VFAs as a carbon source. This may include multiphasic growth patterns and substrate inhibition at concentrations ≥ 2.0 g·L$^{-1}$ (Leonhardt et al., 2026). Since no inhibitory or multiphasic growth behaviour was observed below 2.0 g·L$^{-1}$ total VFA concentration, growth in this range was assumed to be limited primarily by substrate availability and was therefore described using Monod kinetic model.

As shown in Figure 3A the Monod kinetic model accurately described the relationship between microbial growth rate and VFA concentration with a $R^2$ value of 0.998. This implies that, within the investigated concentration range, an increase in $c_{VFA}$ leads to an improvement in $\mu_{app}$. However, as previously mentioned, elevated VFA concentrations may trigger multiphasic growth behaviour and substrate inhibition. In continuous cultivation processes, such effects could lead to the accumulation of less-preferred VFAs and reduce process robustness. Therefore, a target VFA concentration of 0.5 $g \cdot L^{-1}$ was selected for the perfusion process to ensure operation within a non-inhibitory and growth-supporting concentration range. Based on the Monod model, an apparent growth rate of 0.202 $h^{-1}$ is expected at this concentration (Figure 3A).

It should be noted that the kinetic model in Figure 3A was determined with a surplus of ammonium ($NH_4^+ = 2.0\ g \cdot L^{-1}$). Since ammonium concentrations may vary during the perfusion cultivation, the influence of ammonium availability onto growth rate was investigated separately.

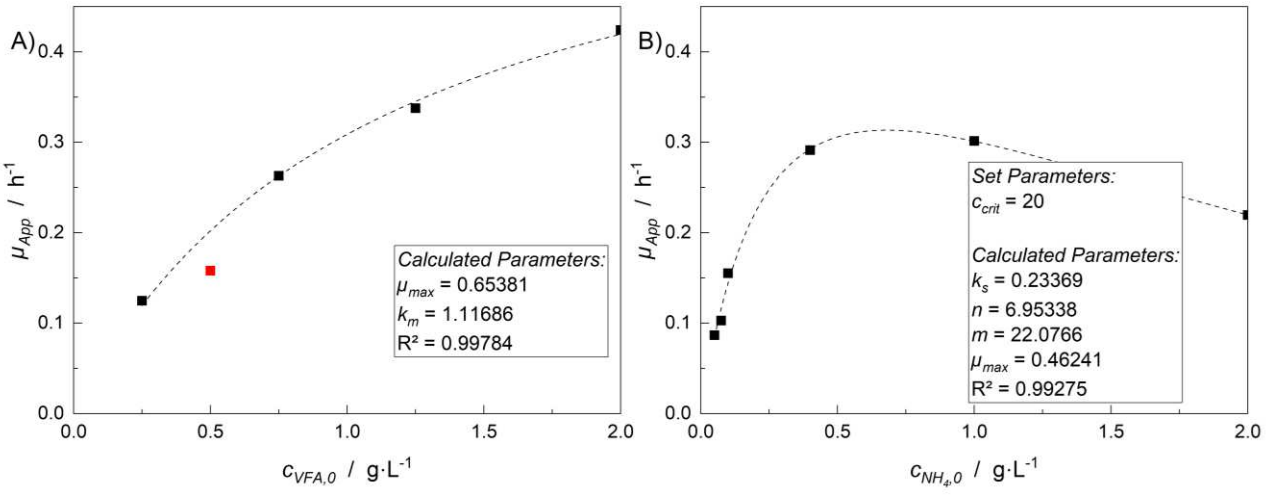


*Figure 3 Influence of A) VFA concentration onto $\mu_{App}$, modeled by monod kinetics and B) ammonium concentration with fitted Han-Levenspiel inhibitory kinetics. The outlier has been marked red.*

As observed in Figure 3-B, a slight inhibitory effect of ammonium was observed at concentration above 1.0 $g \cdot L^{-1}$. To quantitatively describe this behavior, the Han-Levenspiel inhibition model was fitted to the experimental data. The model provided an excellent fit, with an $R^2$ value of 0.9928. The model predicts a maximum growth rate of 0.317 $h^{-1}$ at 0.67 $g \cdot L^{-1}$ of ammonium, indicating a narrow optimum between ammonium limitation and inhibition. Growth remained above 90% of $\mu_{max}$ up to approximately 1.25 $g \cdot L^{-1}$ of $NH_4^+$. In contrast, a pronounced reduction in growth rate was observed below the optimum (As seen in Figure 3B), highlighting the sensitivity of *C. necator* H16 to nitrogen limitation during biomass production.

It should be noted that backscatter measurements do not distinguish between biomass growth and intracellular PHA accumulation. Consequently, the fitted kinetics describe total biomass accumulation rather than biomass gain by cell division. This limitation is expected to be most relevant at low ammonium concentrations, where nitrogen limitation can trigger PHA biosynthesis (Steinbüchel and Füchtenbusch, 1998). Thus, the resulting growth kinetic may lack in precision at very low levels of ammonium. In contrast, cultures supplied with sufficient ammonium are expected to exhibit predominantly growth-associated increases in backscatter. Since all experiments investigation ammonium related effects were conducted at a VFA concentration of 0.5 $g \cdot L^{-1}$, VFA substrate inhibition effects are unlikely to influence the observed trends. Therefore, while the decline in $\mu_{App}$ at low ammonium concentrations may partly reflect increased PHA accumulation, the inhibitory effect observed at elevated ammonium concentrations likely represents a genuine reduction in growth rate.

Despite these limitations, the presented kinetic analysis provided important design parameters for the subsequent perfusion process. The Monod-type relationship between VFA concentration and apparent growth rate confirmed that operation at 0.5 $g \cdot L^{-1}$ VFA maintains the culture within a growth-supporting, non-inhibitory concentration range while minimizing the risk of substrate accumulation and multiphasic growth behaviour. Furthermore, the ammonium inhibition study

demonstrated that *C. necator H16* tolerates substantial variations in $NH_4^+$ concentration without pronounced reductions in apparent growth rate. As a result, moderate fluctuations in ammonium concentration that may occur during perfusion operation are not expected to negatively impact process performance.

### 4.3 Perfusion Process in 3.2-L Scale Bioreactor

A continuous process with cell retention (perfusion) was developed in order to produce PHA from low concentrated VFA stream in a comparatively small reactor volume. The mixture of VFAs used in this set-up was extensively characterised in a previous study (Leonhardt et al., 2026) with the composition being inspired by acidified waste streams from wastewater treatment plants (Prakash et al., 2024). During growth phase, the feed stream contained all nutrients needed for growth, including 20 $g \cdot L^{-1}$ total VFA and 2.85 $g \cdot L^{-1}$ $NH_4^+$ (pH 7.5). During production phase, ammonium was completely removed from the feed medium and pH was increased to 8.0.

Membrane fouling was not observed during the cultivation, as indicated by the stable transmembrane pressure shown in Figure 4B. The maximum permeate flow rate reached 9.7 $mL \cdot min^{-1}$, remaining well below the previously determined critical permeate flow rate of 31.7 $mL \cdot min^{-1}$ for the filter in use (see results 4.1). This confirms that operation below the critical flux successfully prevented membrane fouling during long-term cultivation

To maintain stable membrane operation, a retentate recirculation flow rate of 4 $L \cdot min^{-1}$ was applied, corresponding to a *Reynolds number* of approximately 2500 within the membrane channels. This high recirculation rate generated two notable process effects. First, the returning retentate stream substantially improved mixing within the bioreactor, suggesting that

conventional stirrer-based agitation may contribute less to mixing than in standard cultivation systems.

Second, the recirculation loop introduced a high energy dissipation in the bioreactor, leading to increased heat generation and a higher cooling duty. Unfortunately, this high energy demand for cooling reduces economic feasibility in larger scales. Although reducing the retentate flow rate could lower energy consumption, it would also decrease turbulence within the membrane channels and may promote fouling. Thus, a trade-off exists between membrane performance and energy efficiency.

The benefits of operating below the critical flux become apparent when compared with the work of Kacanski et al. (2022), who reported a continuous increase in transmembrane pressure during perfusion cultivation. However, critical flux was not investigated by Kacanski et al. (2022). Such an increase is typically associated with progressive membrane fouling and may compromise process stability during extended operation.

The whole cultivation profile of the perfusion process is shown in Figure 4. After a process time of 13 h, feed medium was switched to ammonium deficient production medium. Consequently, a sharp decrease in $NH_4^+$ over the following 2 h was observed until complete ammonium depletion in the medium (see also Figure 4B). This effect is mainly attributed to $NH_4^+$ uptake by the culture and wash out due to perfusion. As long as $NH_4^+$ (during growth phase) was present in the culture broth, exponential growth of biomass with an $\mu_{App}$ of $0.249 \pm 0.002\ h^{-1}$ was observed. With the onset of ammonium depletion at 14.5 h, growth of total biomass $c_X$ appeared linear as the culture allocates more of the substrate taken up to PHA production. This behaviour is often seen in PHA fermentation system with separated growth and production phases. As PHA granules grow within the bacteria their size increases linearly, as also demonstrated by Kamasaka et al. (2025).

Figure 4A shows that the concentration of total VFA strongly fluctuates during growth phase (white background) while VFA concentration remains low, but more constant, during production phase (grey background). The higher variance of VFA during growth phase are caused by the OUR triggered medium pulses. While ammonium is present, these pulses are necessary as the uptake of $NH_4^+$ releases $H^+$ into the cultivation broth, thus working against the principle of the VFA feeding strategy by pH-stat.

With the following transition to production phase, pH was adjusted to pH 8 with NaOH. However, with this shift we observed a decrease of VFA concentration to 0.07 ± 0.03 $g \cdot L^{-1}$, thus being substantially lower compared to growth phase. This behavior can be explained by the interaction between the pH-stat feeding strategy and the OUR-triggered feed pulses employed during the growth phase.

During the growth phase, OUR-triggered feed pulses were used to restore the VFA concentration to the target range of $0.5\ g \cdot L^{-1}$. However, $NH_4^+$ assimilation releases protons into the cultivation broth, partially compensating for the increase in pH caused by VFA consumption. Consequently, less VFA was supplied via the pH-stat controller than was actually consumed by *C. necator H16*, causing the residual VFA concentration to gradually decrease between consecutive feed pulses. Once ammonium limitation was reached, OUR-triggered feed pulses ceased because growth-associated oxygen consumption decreased substantially. As a result, the process entered the production phase at a residual VFA concentration that depended on the timing of the final feed pulse rather than on a defined process setpoint. Consequently, the remaining VFA concentration at the onset of nitrogen limitation could theoretically range between 0 and 0.5 $g \cdot L^{-1}$. This explains the low average residual VFA concentrations observed during the production phase.

While the feeding strategy successfully kept the feeding below the critical VFA concentration of 2.0 $g \cdot L^{-1}$, a better control of VFA concentration may lead to a substantially higher growth

rate, as shown by the initial kinetic studies. This lack of control of exact VFA concentrations is especially present during the transition from growth to production. Future process designs should therefore incorporate an improved PAT-based control strategy to maintain VFA concentrations within a predefined target range throughout the production phase.

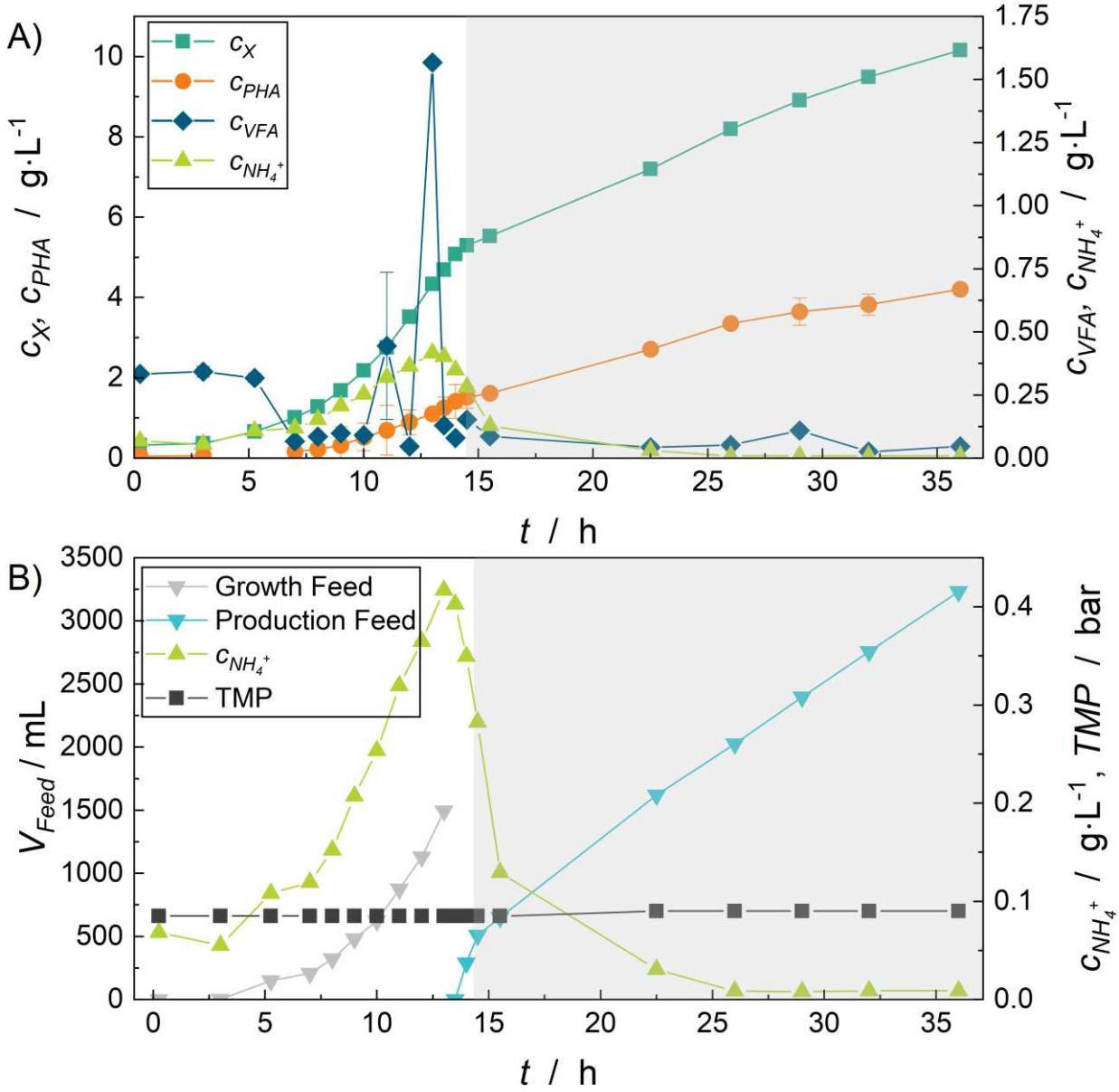


*Figure 4 Time course of Biomass, PHA and fed Volumes in a perfusion process. The process can be divided into a growth phase (0-13.5 h) and an ammonium-deficient production phase (13.5-36 h)*

## 4.4 Comparison of Perfusion Fed-Batch and Batch Cultivation process performance

To evaluate the performance of the developed perfusion strategy, key bioprocess parameters were compared with those obtained in previously reported fed-batch cultivations on the same VFA mixture (Table 3). The biological behaviour of cultivations differs in perfusion and fed-batch mode, due to better supply of micronutrients, and washing out of potentially toxic by-products in perfusion.

As shown in Table 3, the apparent growth rate ($\mu_{App}$) during growth phase increased from 0.204 ± 0.001 $h^{-1}$ in fed-batch cultivation to 0.249 ± 0.002 $h^{-1}$ in perfusion mode, corresponding to an increase of approximately 22%. This observation indicates that continuous medium exchange provided a more favourable environment for biomass formation.

In contrast, $Y_{X/S}$ drastically decreased by 21 % from 0.58 ± 0.01 $g \cdot g^{-1}$ in fed-batch cultivation to 0.46 ± 0.02 $g \cdot g^{-1}$ in perfusion mode. Since comparable residual VFA concentrations were observed during the growth phase, this reduction cannot readily be explained by differences in substrate availability. Instead, it may be related to process-specific factors such as increased shear stress caused by the high retentate recirculation rates or differences in dissolved oxygen concentrations between the two cultivation systems. Both factors may affect cellular metabolism and increase maintenance energy requirements, thereby reducing biomass yields.

*Table 3 Bioprocess characteristics of perfusion cultivation on VFA compared to data published (2026) on the same carbon source in fed-batch. The relevant parameters fed-batch, due-to pH shift in perfusion after growth phase are marked light grey*

| **Reference** | **Leonhardt et al., 2026** | | **This work** |
|---|---|---|---|
| **Process** | **Fed batch** | **Fed batch** | **Perfusion** |
| **pH** | **7.5** | **8.0** | |
| $\mu_{App}$ / $h^{-1}$ | 0.204±0.001 | 0.121±0.005 | 0.249±0.002 |

| | | | |
|---|---|---|---|
| $Y_{X/S}$ / g·g$^{-1}$ | 0.58±0.01 | 0.54±0.05 | 0.46±0.02 |
| $Y_{X/N4+}$ / g·g$^{-1}$ | 4.6±0.2 | 3.7±0.5 | 4.4±0.3 |
| $Y_{P/S}$ / g·g$^{-1}$ | 0.51±0.02 | 0.53±0.02 | 0.26±0.01 |
| *3-HV content* / % | 22.9 | 8.9 | 9.6 |
| $c_{VFA,R,Growth}$ / g·L$^{-1}$ | 0.3±0.5 | 0.5±0.4 | 0.3±0.4 |
| $c_{VFA,R,Production}$ / g·L$^{-1}$ | 1.3±0.7 | 0.4±0.3 | 0.07±0.03 |
| $pO_{2,mean}$ / % | 20 % | 20 % | >50 % |

435

436 The impact of perfusion cultivation became even more apparent during the production phase.
437 While a $Y_{P/S}$ of 0.53 g·g$^{-1}$ was achieved in the fed-batch fermentation at pH 8.0, the
438 corresponding value in the present study decreased by approximately by 51 % to 0.26±0.01 g·g$^{-}$
439 $^{1}$. This reduction corresponded with a substantially lower residual VFA concentration during
440 the production phase (0.07 ± 0.03 g·L$^{-1}$ compared with 0.4 ± 0.3 g·L$^{-1}$ in fed-batch cultivation),
441 suggesting that the culture experienced carbon-limited conditions. In *C. necator H16*, low
442 concentrations of substrate have previously been reported to negatively affect PHA
443 accumulation on butyric acid by Shimizu et al. (1993). Under such substrate-limited conditions,
444 a larger fraction of the supplied carbon is expected to be diverted towards cellular maintenance
445 and essential cellular functions rather than PHA synthesis. This interpretation is supported by
446 the relatively low biomass-specific production rate $q_P$ of 0.025 ± 0.002 g·g$^{-1}$·h$^{-1}$ observed during
447 the production phase, thus indicating limited conversion of substrate into intracellular polymer.
448 These findings suggest that maintaining residual VFA concentrations above a critical threshold
449 is essential to sustain high PHA synthesis rates and maximize substrate-to-product conversion
450 efficiency in fed-batch operation.

451 Despite these limitations, increasing the residual VFA concentration is not straightforward.
452 Previous work demonstrated that mixed VFA concentrations exceeding approximately 2.0 g·L$^{-}$

[1] can induce multiphasic growth behaviour and substrate inhibition (Leonhardt et al., 2026). Therefore, the operational window for continuous feeding of mixed VFAs remains relatively narrow, requiring a compromise between sufficient substrate availability for PHA synthesis and avoidance of inhibitory effects. Tighter process control and better understanding of the process e. g. by process simulation may help to optimize the exploitation of this operational window.

The studies summarized in Table 4 demonstrate that the raw material efficiency achieved in the present work is comparable to that reported for other perfusion and semi-continuous cultivations but lower than that of several batch cultivations. This can be attributed to two factors: First, lower residual VFA concentrations during the production phase results in decreased PHA yields on substrate, as Shimizu et al. (1993) also reported that a higher residual VFA concentrations is preferred during the production phase to achieve higher PHA yield. Second, perfusion processes inherently lose a fraction of the supplied substrate through the continuous removal of spent medium, which also contains unconsumed VFAs.

*Table 4 Comparison of process performance of reported PHA production from low concentrated VFAs. [a]Values are calculated from published data*

| | **Mode** | **Titer / $g \cdot L^{-1}$** | **Productivity / $g \cdot L^{-1} \cdot h^{-1}$** | **Raw Material Efficiency / $g_{PHA} \cdot g_{VFA}^{-1}$** |
|---|---|---|---|---|
| **Vu et al. (2022)** | Batch | 1.5 | 0.04[a] | 0.32 [a] |
| **Al Battashi et al. (2021)** | Batch | 1.94±0.07 | 0.04 | 0.19 ± 0.01 |
| **Vu et al. (2023)** | Semi-continuous | 2.8 | 0.02 [a] | 0.13 [a] |
| **Kacanski et al. (2022)** | Perfusion | 12.24 | 0.17 [a] | - |
| **This work** | Perfusion | 4.2±0.2 | 0.12 | 0.13 |

Nevertheless, perfusion cultivation offers a clear advantage with respect to higher product titers and higher productivities (see Table 4), as batch processes are majorly limited by the toxicity of VFAs. While the batch cultivation reached final PHA concentrations below 2 $g \cdot L^{-1}$, these processes are majorly limited by the toxicity of VFAs. However, the perfusion mode used in this work reached a PHA concentration of 4.2±0.2 $g \cdot L^{-1}$. These improvements are primarily attributable to continuous substrate feeding combined with cell retention, which allows feeding the VFA below the toxic concentration range.

On the other side, Kacanski et al. (2022) presented a perfusion method using acetic acid as a carbon source for PHA production in *Bacillus megaterium uyuni S29*. As Kacanski et al. (2022) used pure acetic acid instead of a VFA mixture, higher substrate concentrations are possible, as no multiphasic patterns are expected to occur. Thus, the used acetic acid enables higher PHA production with a final titer of 12.24 $g \cdot L^{-1}$. Additionally, an earlier study revealed that pure acetic acid is less toxic than other organic acids (Leonhardt et al., 2025) and less toxic than VFA mixture (Leonhardt et al., 2026). Consequently, substantially higher substrate concentrations can be maintained without impairing cellular performance, enabling higher biomass and PHA titers when acetic acid is used as sole carbon source.

# 5 Conclusion

This work provides a streamlined process development, successfully demonstrating a perfusion strategy for the production of PHA using *Cupriavidus necator H16*. The results show the performance of the implemented ceramic membrane and systematically investigate cell growth and PHA production in a kinetical study. Thus, a perfusion process was established converting

491 a low concentrated feed of 20 g·L$^{-1}$ (95 g VFA) into 10.2 g·L$^{-1}$ (32 g) of Biomass, containing
492 4.2 g·L$^{-1}$ (13.4 g) of PHA.

493 The application of tangential flow filtration (TFF) enabled stable cell retention throughout
494 cultivation and demonstrated the successful implementation of membrane-assisted perfusion
495 processing. Owing to the systematic determination of the critical flux, no significant membrane
496 fouling was observed during operation, underlining the robustness of the selected ceramic
497 membrane system. Nevertheless, the process remained associated with elevated energy demand
498 caused by pumping requirements due to continuous recirculation through the filter, which
499 represents an important aspect for future process optimization and scale-up considerations.

500 The kinetic investigations further revealed only minor inhibitory effects of ammonium
501 concentrations below 2.0 g·L$^{-1}$, whereas the biomass growth rate exhibited pronounced
502 sensitivity toward changes in VFA concentration. Additionally, the findings of this study
503 suggest a major influence of VFA concentration onto PHA production rate which needs to be
504 further evaluated.

505 Consequently, the adapted pH-OUR control strategy based on the approach proposed by
506 Huschner et al. (2015) enabled extended process operation. However, the feeding strategy did
507 not consistently maintain VFA concentrations at the target of 0.5 g·L$^{-1}$, limiting overall process
508 performance. These findings emphasize the importance of advanced monitoring and control
509 strategies for future process intensification. In this context, the implementation of real-time
510 analytical tools, such as Raman spectroscopy or ATR-FTIR-based monitoring (Christie et al.,
511 2024), could enable improved regulation of VFA concentrations and thereby enhance process
512 stability and productivity. Furthermore, the pronounced sensitivity of the system toward VFA
513 concentrations suggests that substrate gradients may become increasingly critical during scale-
514 up, where insufficient mixing could strongly influence cellular performance and overall process
515 robustness.

Overall, this study demonstrates how integrated membrane characterization and biological process understanding can support rational perfusion process development for PHA production. The generated process knowledge provides an important basis for future optimization, particularly regarding the influence of process parameters and fluctuating feed compositions on key process performance indicators, including titer, rate, and yield.

## 6 Ethics approval and consent to participate

Not applicable

## 7 Consent for publication

Not applicable

## 8 Availability of data and material

Data will be made available at request.

## 9 Competing interests

The authors declare that there are no financial or non-financial competing interests that could have influenced the work reported in this paper.

## 10 Funding

We would like to thank the Baden-Württemberg Ministry of the Environment, Climate Protection and the Energy Sector and the European Union for funding the project "KoalAplan" as part of the ERDF (European Regional Development Fund) programme "Bioeconomy - Biorefineries for the recovery of raw materials from waste and wastewater" (Grant No.: Bioök_2076393).

Additionally, we would like to thank the Baden-Württemberg Ministry of the Environment, Climate Protection and the Energy Sector, and the European Union for funding the project “BW2Pro” as part of the ERDF (European Regional Development Fund) program

"Bioeconomy–Biorefineries for the recovery of raw materials from waste and wastewater" (Grant No.: Bioök_2275052 and Bioök_2076199).

And finally, we would like to thank the German Federal Ministry of Agriculture, Food and Regional Identity (BMELH) for funding the project "PolyDiTex" (Grant No.: 223NR059B and 223NR059C).

## 11 Acknowledgement

We would like to thank the research group of Professor Harald Horn from Karlsruhe Intitute of Technology, Germany for coordinating the researchproject KoalAplan and providing us with a VFA rich feedstock for analysis.

## 12 Author contributions

Steven Leonhardt: Conceptualization (lead), Investigation (lead), Methodology, Formal Analysis, Writing – Original Draft Preparation (lead);

Birk Achenbach: Conceptualization, Methodology, Investigation, Writing – Review & Editing;

Pravesh Tamang: Conceptualization, Project Administration, Supervision, Writing – Review & Editing;

Alexander Beck: Conceptualization, Methodology, Writing – Review & Editing;

Günter E. M. Tovar: Supervision, Writing - Review & Editing;

Susanne Zibek: Project Administration, Funding Acquisition, Supervision (lead), Writing – Review & Editing.

# 13 References


Achenbach, B., Tamang, P., Leonhardt, S., Tovar, G.E.M., Zibek, S., 2026. Controlled Feeding Facilitates the Development of a Robust Production Process for Terpolymeric Polyhydroxyalkanoates. Biotechnology journal 21, e70252. https://doi.org/10.1002/biot.70252.

Agrawal, P., Wilkstein, K., Guinn, E., Mason, M., Serrano Martinez, C.I., Saylae, J., 2023. A Review of Tangential Flow Filtration: Process Development and Applications in the Pharmaceutical Industry. Org. Process Res. Dev. 27, 571–591. https://doi.org/10.1021/acs.oprd.2c00291.

Al Battashi, H., Al-Kindi, S., Gupta, V.K., Sivakumar, N., 2021. Polyhydroxyalkanoate (PHA) Production Using Volatile Fatty Acids Derived from the Anaerobic Digestion of Waste Paper. J Polym Environ 29, 250–259. https://doi.org/10.1007/s10924-020-01870-0.

Arnaud, J.P., Lacroix, C., Foussereau, C., Choplin, L., 1993. Shear stress effects on growth and activity of Lactobacillus delbrueckii subsp. bulgaricus. Journal of biotechnology 29, 157–175. https://doi.org/10.1016/0168-1656(93)90048-R.

Baranyi, J., Pin, C., 1999. Estimating bacterial growth parameters by means of detection times. Applied and environmental microbiology 65, 732–736. https://doi.org/10.1128/aem.65.2.732-736.1999.

Beck, A., Vogt, F., Hägele, L., Rupp, S., Zibek, S., 2022. Optimization and Kinetic Modeling of a Fed-Batch Fermentation for Mannosylerythritol Lipids (MEL) Production With Moesziomyces aphidis. Frontiers in bioengineering and biotechnology 10, 913362. https://doi.org/10.3389/fbioe.2022.913362.

Cai, F., Lin, M., Jin, W., Chen, C., Liu, G., 2023. Biosynthesis of poly(3-hydroxybutyrate-co-3-hydroxvalerate) from volatile fatty acids by Cupriavidus necator. Journal of basic microbiology 63, 128–139. https://doi.org/10.1002/jobm.202200448.

584 Cheah, Y.-K., Vidal-Antich, C., Dosta, J., Mata-Álvarez, J., 2019. Volatile fatty acid
585 production from mesophilic acidogenic fermentation of organic fraction of municipal solid
586 waste and food waste under acidic and alkaline pH. Environmental science and pollution
587 research international 26, 35509–35522. https://doi.org/10.1007/s11356-019-05394-6.
588 Chmiel, H., Takors, R., Weuster-Botz, D. (Eds.), 2018. Bioprozesstechnik, 4th ed. Springer
589 Spektrum, Berlin, Heidelberg, 585 pp.
590 Christie, L., Rutherford, S., Palmer, D.S., Baker, M.J., Butler, H.J., 2024. Bioprocess
591 monitoring applications of an innovative ATR-FTIR spectroscopy platform. Frontiers in
592 bioengineering and biotechnology 12, 1349473.
593 https://doi.org/10.3389/fbioe.2024.1349473.
594 Doran, P., 1995. Bioprocess Engineering Principles. Elsevier.
595 Espinasse, B., Bacchin, P., Aimar, P., 2002. On an experimental method to measure critical
596 flux in ultrafiltration. Desalination 146, 91–96. https://doi.org/10.1016/S0011-
597 9164(02)00495-2.
598 Han, K., Levenspiel, O., 1988. Extended monod kinetics for substrate, product, and cell
599 inhibition. Biotechnology and bioengineering 32, 430–447.
600 https://doi.org/10.1002/bit.260320404.
601 Huschner, F., Grousseau, E., Brigham, C.J., Plassmeier, J., Popovic, M., Rha, C., Sinskey,
602 A.J., 2015. Development of a feeding strategy for high cell and PHA density fed-batch
603 fermentation of Ralstonia eutropha H16 from organic acids and their salts. Process
604 Biochemistry 50, 165–172. https://doi.org/10.1016/j.procbio.2014.12.004.
605 Jawed, K., Irorere, V.U., Bommareddy, R.R., Minton, N.P., Kovács, K., 2022. Establishing
606 Mixotrophic Growth of Cupriavidus necator H16 on CO2 and Volatile Fatty Acids.
607 Fermentation 8, 125. https://doi.org/10.3390/fermentation8030125.

608 Jiang, J., Zhang, Y., Li, K., Wang, Q., Gong, C., Li, M., 2013. Volatile fatty acids production
609 from food waste: effects of pH, temperature, and organic loading rate. Bioresource
610 technology 143, 525–530. https://doi.org/10.1016/j.biortech.2013.06.025.
611 Kacanski, M., Pucher, L., Peral, C., Dietrich, T., Neureiter, M., 2022. Cell Retention as a
612 Viable Strategy for PHA Production from Diluted VFAs with Bacillus megaterium.
613 Bioengineering (Basel, Switzerland) 9. https://doi.org/10.3390/bioengineering9030122.
614 Kamasaka, K., Abekawa, N., Takeda, K., Noi, K., Matsuda, M., Matsumoto, K., Yumoto, N.,
615 Kondo, A., Hasunuma, T., 2025. Monitoring proliferation and material production of
616 Cupriavidus necator H16 using cell count and volume measurement. Scientific reports 15,
617 30416. https://doi.org/10.1038/s41598-025-16567-4.
618 Leonhardt, S., Achenbach, B., Tamang, P., Tovar, G.E.M., Zibek, S., 2026. Increasing pH
619 leads to more efficient production of polyhydroxyalkanoates from volatile fatty acids
620 using Cupriavidus necator H16. Microbial cell factories 25.
621 https://doi.org/10.1186/s12934-026-03135-2.
622 Leonhardt, S., Tamang, P., Tovar, G.E.M., Zibek, S., 2025. Characterizing the growth of
623 PHA-producing microorganisms on short-chain carboxylic acids. Microbial cell factories
624 24, 206. https://doi.org/10.1186/s12934-025-02840-8.
625 Makkar, N.S., Casida, L.E., 1987. Cupriavidus necator gen. nov., sp. nov; a Nonobligate
626 Bacterial Predator of Bacteria in Soil. International Journal of Systematic Bacteriology 37,
627 323–326. https://doi.org/10.1099/00207713-37-4-323.
628 Monod, J., 1949. THE GROWTH OF BACTERIAL CULTURES. Annu. Rev. Microbiol. 3,
629 371–394. https://doi.org/10.1146/annurev.mi.03.100149.002103.
630 Prakash, N.S., Maurer, P., Horn, H., Hille-Reichel, A., 2024. Valorization of organic carbon
631 in primary sludge via semi-continuous dark fermentation: First step to establish a
632 wastewater biorefinery. Bioresource technology 397, 130467.
633 https://doi.org/10.1016/j.biortech.2024.130467.

634 Shimizu, H., Tamura, S., Shioya, S., Suga, K., 1993. Kinetic study of poly-d(−)-3-
635 hydroxybutyric acid (PHB) production and its molecular weight distribution control in a
636 fed-batch culture of Alcaligenes eutrophus. Journal of Fermentation and Bioengineering
637 76, 465–469. https://doi.org/10.1016/0922-338X(93)90242-Z.
638 Steinbüchel, A., Füchtenbusch, B., 1998. Bacterial and other biological systems for polyester
639 production. Trends in biotechnology 16, 419–427. https://doi.org/10.1016/S0167-
640 7799(98)01194-9.
641 Velghe, F., Wilde, F. de, Snellinx, S., Farahbakhsh, S., Belderbos, E., Peral, C., Wiedemann,
642 A., Hiessl, S., Michels, J., Pierrard, M.-A., Dietrich, T., 2021. Volatile fatty acid platform
643 - a cornerstone for the circular bioeconomy. FEMS microbiology letters 368.
644 https://doi.org/10.1093/femsle/fnab056.
645 Vu, D.H., Mahboubi, A., Root, A., Heinmaa, I., Taherzadeh, M.J., Åkesson, D., 2022.
646 Thorough Investigation of the Effects of Cultivation Factors on Polyhydroalkanoates
647 (PHAs) Production by Cupriavidus necator from Food Waste-Derived Volatile Fatty
648 Acids. Fermentation 8, 605. https://doi.org/10.3390/fermentation8110605.
649 Vu, D.H., Mahboubi, A., Root, A., Heinmaa, I., Taherzadeh, M.J., Åkesson, D., 2023.
650 Application of Immersed Membrane Bioreactor for Semi-Continuous Production of
651 Polyhydroxyalkanoates from Organic Waste-Based Volatile Fatty Acids. Membranes 13.
652 https://doi.org/10.3390/membranes13060569.
653 Wang, J., Yue, Z.-B., Sheng, G.-P., Yu, H.-Q., 2010. Kinetic analysis on the production of
654 polyhydroxyalkanoates from volatile fatty acids by Cupriavidus necator with a
655 consideration of substrate inhibition, cell growth, maintenance, and product formation.
656 Biochemical Engineering Journal 49, 422–428. https://doi.org/10.1016/j.bej.2010.02.005.
657 Yu, J., Si, Y., 2004. Metabolic carbon fluxes and biosynthesis of polyhydroxyalkanoates in
658 Ralstonia eutropha on short chain fatty acids. Biotechnology progress 20, 1015–1024.
659 https://doi.org/10.1021/bp034380e.

660

## Supplementary Files

This is a list of supplementary files associated with this preprint. Click to download.

- 261111GraphicalAbstractPerfusion.png